Experimental verification of semiclassical and RPA calculations of the static conductivity in moderately nonideal plasmas

Y. Vitel and M. El Bezzari
Laboratoire des Plasmas Denses, Université Pierre et Marie Curie, Tour 12 E 5, 4 Place Jussieu, 75252 Paris Cedex 05, France

A. A. Mihajlov
Institute of Physics, P.O. Box 57, 11001 Belgrade, Yugoslavia

Z. Djurić
Department of Materials, Oxford University, Parks Road, Oxford OX1 3PH, United Kingdom

(Received 12 July 2000; published 24 January 2001)

We present an experimental verification of the semiclassical theory for static conductivity calculations in the case of moderately nonideal plasmas. Such plasmas are produced in linear flashlamps filled with pure helium and are characterized by on axis electron densities in the range 2×10^{17}–1.7×10^{18} cm^{-3} and temperatures $(2-3)\times10^4$ K. Precise measurements of the discharge electrical parameters have been carried out and in each case the impedance of the plasma was compared with the calculated value using the semiclassical theory, which is a simpler approximation than the quantum-mechanical theory based on the random-phase approximation.

DOI: 10.1103/PhysRevE.63.026408 PACS number(s): 52.25.Fi

I. INTRODUCTION

We present an experimental verification of the semiclassical theory [1] for static conductivity calculations in the case of moderately nonideal plasmas, which was developed as a simpler approximation than the quantum-mechanical theory based on the random-phase approximation (RPA) [2,3]. Such plasmas are produced in linear flashlamps filled with pure helium and are characterized by on axis electron densities in the range $2\times10^{17}-1.7\times10^{18}$ cm^{-3} and at temperatures around $(2-3)\times10^4$ K. In these conditions, the mean interaction potential energy between charged particles, E_p, is appreciable compared to their kinetic energy E_k. The coupling parameter defined as $\Gamma=E_p/E_k$ is in the range 0.1–0.2 [4]. Those pulsed arcs have a good cylindrical symmetry, and are reproducible and in local thermodynamic equilibrium. Different methods of diagnostics based on measurements of continuum intensities, neutral line intensities, and opacities (taking into account the effect of the statistical ionic microfields on the atomic levels), and infrared laser interferometry (3.39 mm), are applied to determine the radial profiles of particles and temperature. Such experimental conditions coupled with precise measurements of the discharge electrical parameters (current intensity and electrical field) allow for a reliable evaluation of the validity of this semiclassical theory. Finally, for each case, the impedance of the plasma so calculated is in good agreement with the experimental value, proving the validity of the semiclassical theory [1] and thereby of the RPA theory [2,3] in our plasmas.

II. EXPERIMENTAL SETUP AND PLASMA DIAGNOSTICS

A. Experimental setup

This experimental setup is displayed in Fig. 1. The plasmas are produced in fused quartz linear flashlamps whose inner diameter is 5 mm and distance between electrodes 100 mm. These lamps are filled with pure helium at initial pressures from 50 to 500 Torr. The gas breakdown is performed by applying a high voltage pulse (30 kV, 1 μs) on an external auxiliary electrode. Then a low current ($\simeq$1 A) simmer is maintained for 30 ms before triggering the main discharge to ensure a discharge centering around the tube axis. The electrical pulse is produced by means of a LC cell with variable inductance, which permits us to adapt the source impedance to the plasma impedance. The maximum current intensity is set in the range 0.5–1.6 kA and its pulse duration (full width at half maximum) is around 100 μs. The voltage drop across the tube is measured by a precise ($\pm1\%$) voltage divider, and the current intensity by a coaxial shunt ($R=0.25$ m$\Omega\pm0.2\%$) connected to a differential amplifier. Both signals are recorded on a digital oscilloscope and processed by a personal computer. In this way, the temporal evolution of the impedance of the plasma can be deduced, as shown in Fig. 2.

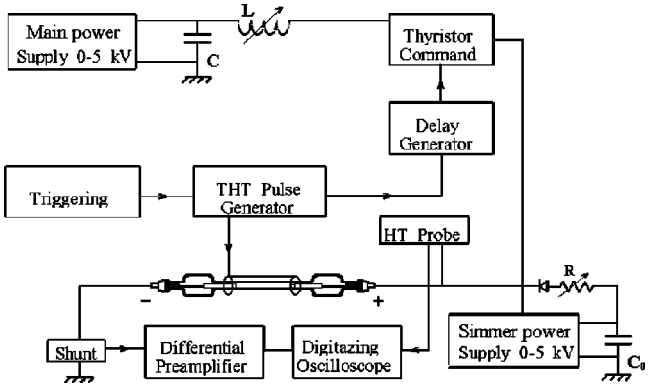

FIG. 1. Experimental setup.

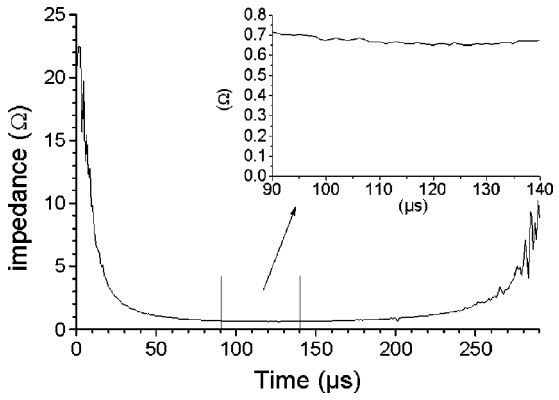

FIG. 2. Temporal evolution of plasma impedance (at the initial pressure 400 Torr).

B. Plasma diagnostics

Different methods of diagnostics are applied to determine the radial profiles of particles and temperature. They are based on optical measurements of the transverse distribution of the continuum intensities (at 780 and 820 nm where the plasma is optically thin) which give the radial functions of the emission coefficient by applying Abel inversion. All those measurements are performed at the maximum discharge current (exposure time around 1 μs) where the best filling of the plasma column inside the tube is obtained. All the details concerning these methods and the determination of the plasma parameters are given in a previous paper [4]. A summary of the main results is given hereafter. The temperatures on axis deduced from the ratio of line intensities to their adjacent continuum on the basis of classical plasma calculations are in disagreement with those deduced from opacity measurements. Their values are by far too high compared to the ones deduced from optical thickness, and would have to lead to the observation of ionic helium lines in the spectra, but we have never seen any. On the other hand, if we take into account the effect of statistical ionic microfields on atomic levels in the calculation of the continuum and line intensities [4,5], a good agreement is obtained in the evaluation of the temperature by both methods, and in the determination of the electron density given by absolute continuum measurements and by infrared laser interferometry. Radial profiles of temperature and electron density so deduced are relatively flat and show a good filling of the plasma inside the flashlamp, as shown in Figs. 3–5 for the extreme discharge energies at each initial gas pressure.

The estimated relative errors of measured temperatures and electron densities are 7% and 5%, respectively. Table I shows the degree of ionization α in the hot region for initial pressures and discharge energies presented in Figs. 3–5, defined as

$$\alpha = \frac{n_e}{n_{at} + n_e}, \tag{1}$$

where n_{at} is the neutral density.

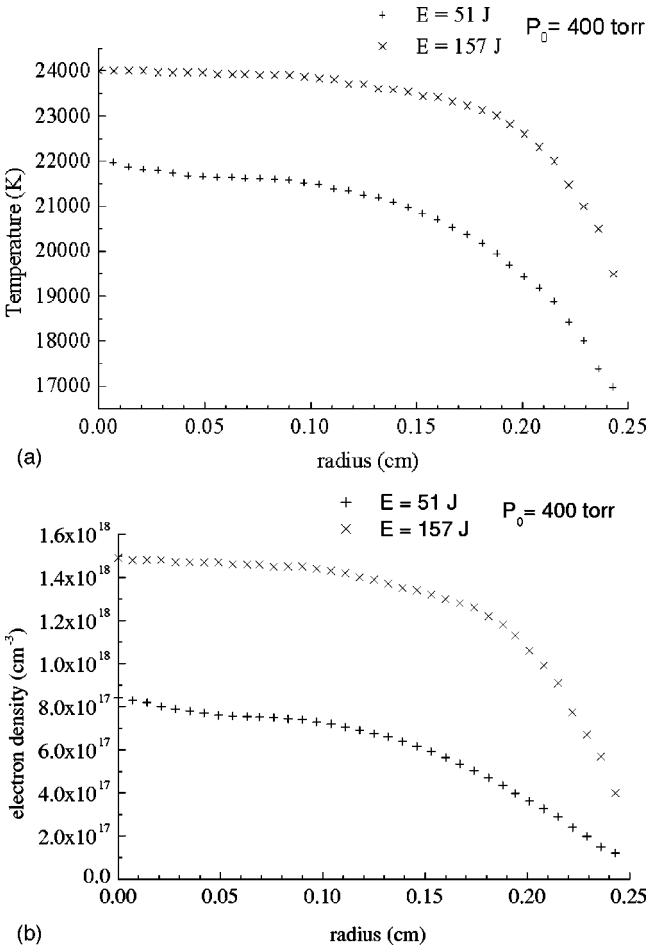

FIG. 3. (a) Radial temperature profile; (b) radial electron density profile. The initial pressure is 400 Torr and discharge energies are 51 J and 157 J.

III. THEORY

The results of the described experiments have enabled us to check the validity of the semiclassical (SC) method [1] of calculating the static electroconductivity of fully ionized plasmas, in domains of electron concentrations N_e and temperature T where the plasma can be treated as singly ionized. Because of that, a semiclassical expression for plasma static conductivity from [1] can be given in a somewhat simplified form:

$$\sigma_{SC} = \frac{8(2kT)^{3/2}}{(\pi m)^{1/2} e^2} \frac{\gamma_{ee}}{\ln\{[1 + (2kTr_c x_0/e^2)^2]^{1/2}\}}, \tag{2}$$

where m and e are the mass and charge of electrons, γ_{ee} is the electron scattering factor, and r_c and x_0 are defined by the relations

$$r_c = q r_d, \quad r_d = (4\pi e^2 N_e/kT)^{-1/2}, \tag{3}$$

$$x_0 = \frac{3}{2} f(p), \quad f(p) = 2.198 - 0.262p. \tag{4}$$

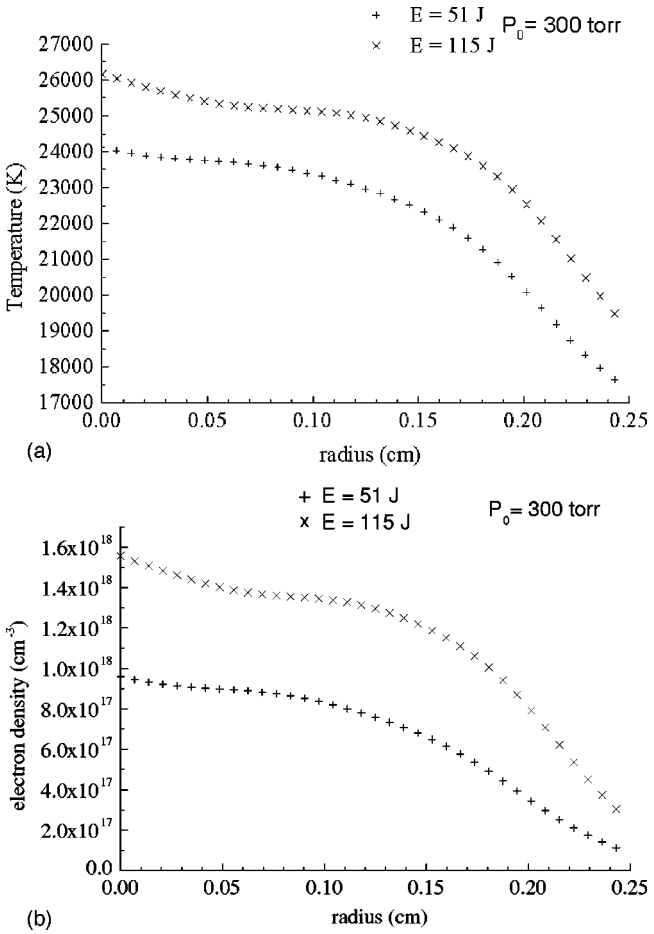

FIG. 4. Same as Fig. 3, but for the initial pressure 300 Torr and discharge energies 51 J and 115 J.

The variable r_c is the screening radius, defined as the product of the Debye screening radius r_d and the corrective factor q, and

$$p = e^2 (kTr_c)^{-1}. \tag{5}$$

The variable p in the last expression represents a plasma nonideality factor, usually denoted in the literature as γ. The letter p is chosen to differ from γ_{ee} used in Eq. (2). In the N_e and T domains under consideration, the values of the electron scattering factor γ_{ee} are very close to that of the well known Spitzer factor γ_E given in [6], and for singly ionized plasma $\gamma_E = 0.582$.

The SC method from [1] for calculating the static conductivity of fully ionized plasmas was chosen not only because of its simplicity and the possibility of interpreting experimental data, but also because it is a good approximation of the RPA method, as elaborated in [2,3]. It was assumed in [2,3] that (i) each particle in a fully ionized plasma moves independently in a homogeneous self-consistent potential field formed by all charged particles; and (ii) the static conductivity of this medium is finite because of the scattering of charged particles with fluctations of that field.

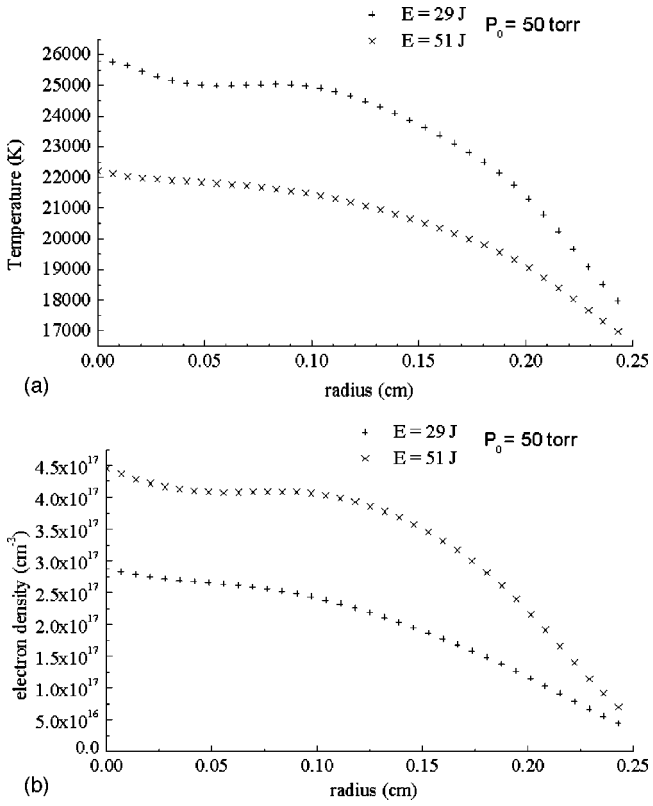

FIG. 5. Same as Fig. 3, but for the initial pressure 50 Torr and discharge energies 29 J and 51 J.

Within the framework of this approach the static conductivity of a fully ionized plasma is given by an expression similar to Lorentz's, namely,

$$\sigma_{RPA} = \frac{4e^2}{3m} \int \rho(E)\tau(E)[-dW(E)/dE]EdE, \tag{6}$$

where E is the free-electron energy, $\rho(E) = (m^3 E/2\pi^4\hbar^6)^{1/2}$ is the density of the free-electron states, $W(E) = \{\exp[\beta(E-\mu_e)]+1\}^{-1}$ is the Fermi-Dirac distribution function, $\beta \equiv (k_B T)^{-1}$, μ_e is the chemical potential of the electron subsystem with temperature T and electron density N_e, and $\tau(E)$ is the relaxation time. In this method $\tau(E)$ is given by the expression

TABLE I. Values of the degree of ionization α [Eq. (1)].

Discharge energy	Initial pressure (Torr)		
(J)	50	300	400
29	0.23		
51	0.62	0.22	0.09
115		0.34	
157			0.16

TABLE II. Experimental and calculated values of impedance (taken at the maximum of the discharge current) as functions of the discharge energy; tube at 50 Torr.

Discharge energy (J)	Z_{expt} (Ω)	Z_{SC_q} (Ω)	Z_{SC_1} (Ω)	Z_{Kur} (Ω)	Z_{Spitz} (Ω)
28	0.71	0.65	0.62	0.57	0.53
39	0.60	0.57	0.55	0.50	0.47
50	0.52	0.53	0.51	0.46	0.43

$$\tau(E)=1/\nu(E),$$

$$\nu(E)=\frac{4\pi m e^4}{\beta(2mE)^{3/2}}\int_0^{(8mE)^{1/2}/\hbar}\frac{dq}{q}\sum_{\nu}\frac{\chi_e\Pi_{e\nu}+\chi_i\Pi_{i\nu}}{\varepsilon_\nu^3(q)}, \tag{7}$$

where $\nu(E)$ is the electron scattering frequency, which contains the basic information about inner plasma interactions. χ_e and χ_i are the electron and ion form factors, while ε_ν, $\Pi_{e\nu}$, and $\Pi_{i\nu}$ are the dielectric permeability and electronic and ionic polarization operators. The subscript ν refers to the Matsubara frequency, while the summation over ν is carried out in the manner described in [3]. Equation (7) was deduced from perturbation theory for the temperature Green functions, using the Brueckner method of partial summing of infinite sequences of the diagrams containing polarization loops. The final expression suggests that (i) the charged particle's contribution to the self-consistent field is described by the screened Coulomb potential; and (ii) the dielectric function, which defines the charge screening, and the charge-charge static structure factor, characterizing the correlation effects in the charged particles' distribution, are both included in the random-phase approximation.

The expression for the screening radius obtained in the random-phase approximation gives a classical Debye formula in the case of an ideal plasma. For high electron densities it gives the Tomas-Fermi formula for the electron contribution to the total screening.

The calculation of electron scattering amplitudes, which resulted in Eq. (7), is based on Born's approximation. The applicability of this approximation in the case of electron scatterings on the plasma self-consistent field fluctuations is validated by the small parameter s, given by the relation

$$s=\frac{e^2}{\hbar v_T}\frac{\exp(-\kappa a)}{\kappa a}, \tag{8}$$

where $\kappa\sim r_d^{-1}$, $a\sim N_e^{-1/3}$, and the thermal velocity of electrons is $v_T\sim m^{-1/2}T^{1/2}$. In the past, the main objective of the presented RPA method was to study the kinetic properties of plasmas with typical electron densities $N_e\gtrsim 10^{20}$ cm^{-3} and temperatures $T\sim 10^4$ K, formed, for example, in powerful underwater electric discharges. In domains of $N_e\sim 10^{21}$ cm^{-3} and $T\sim 10^4$ K it was shown that the parameter s had a value about 10^{-2}. Results presented here show that the RPA method can be applied for much higher values of s.

TABLE III. Same as Table II, but for tube at 300 Torr.

Discharge energy (J)	Z_{expt} (Ω)	Z_{SC_q} (Ω)	Z_{SC_1} (Ω)	Z_{Kur} (Ω)	Z_{Spitz} (Ω)
50.0	0.62	0.55	0.52	0.48	0.43
61.5	0.57	0.52	0.51	0.47	0.41
74.5	0.53	0.49	0.46	0.45	0.39
89.0	0.50	0.47	0.44	0.43	0.37
105.0	0.46	0.45	0.42	0.39	0.35

It should be emphasized that the above expressions and the classical Spitzer formula do not contain any empirical or semiempirical fitting factors. Nevertheless, we do not know any case where our calculations are in greater discrepancy with experimental results than any other method. It is no wonder that for weakly correlated plasmas, where the classical Spitzer formula is still applicable, the values of conductivity obtained from Eq. (7) are not worse than those found by the Spitzer formula. Regarding the classical Spitzer theory, we would like to underline the following: (i) the screening is included only through the choice of the screening radius as the upper limit of the deviation rates, while the collision rate of electrons is calculated using the Rutherford formula; (ii) no correlation effects in the distribution of charged particles are taken into account. It is worth mentioning that the Born approximation for the scattering cross section coincides with the Rutherford formula for ordinary Coulomb potentials.

In this paper the validity of SC and RPA methods was checked by comparison with experimental results. The accuracy of these methods was also compared with the accuracy of Spitzer's formula [6] and the method developed in [8].

IV. RESULTS AND DISCUSSION

A verification of the semiclassical method was carried out by comparing experimental values of the plasma impedance in a flash lamp (Z_{expt}) with impedance values calculated by the expression (2), taking into account the radial profiles of the plasma parameters. The corrective factor q in Eq. (3) was $q=1$ and $q>1$, and the corresponding impedance values are denoted as Z_{SC_1} and Z_{SC_q}. In the case when $q>1$, this factor was determined from [7]. Tables II–IV show the experimental and calculated values of impedance as functions of the

TABLE IV. Same as Table II, but for tube at 400 Torr.

Discharge energy (J)	Z_{expt} (Ω)	Z_{SC_q} (Ω)	Z_{SC_1} (Ω)	Z_{Kur} (Ω)	Z_{Spitz} (Ω)
50.0	0.65	0.56	0.53	0.48	0.44
61.5	0.56	0.53	0.50	0.46	0.42
74.5	0.54	0.51	0.48	0.44	0.39
89.0	0.50	0.49	0.46	0.43	0.38
105.0	0.47	0.47	0.44	0.41	0.36
120.0	0.45	0.45	0.42	0.39	0.35
140.0	0.43	0.44	0.41	0.38	0.34

TABLE V. Values of RPA conductivity [σ_{RPA}, Eqs. (6) and (7)], in units of $10^4\ \Omega^{-1}\,\mathrm{m}^{-1}$.

T	N_e (cm^{-3})				
(10^4 K)	10^{17}	5×10^{17}	10^{18}	5×10^{18}	10^{19}
1	0.2804	0.3388	0.3721	0.4810	0.5496
1.5	0.4790	0.5624	0.6131	0.7703	0.8653
2	0.7024	0.8114	0.8782	1.087	1.209
2.5	0.9405	1.085	1.165	1.426	1.575
3	1.188	1.381	1.473	1.785	1.963
4	1.703	2.026	2.147	2.553	2.792
5	2.251	2.720	2.890	3.380	3.681

discharge energy. In the domains of electron densities and temperatures of interest here, the calculated values of SC and RPA conductivities are essentially the same, and therefore for the impedance calculations only one method need be used. Since the RPA method is based on rather complicated and lengthy calculations, our choice was the SC method, which can be presented in a closed analytical form, and therefore can serve as a computationally more efficient alternative.

Tables II–IV show that the agreement between the experimental and theoretical results improves with increase of the discharge energy. This is a consequence of the fact that the increase of discharge energy is followed by a significant increase of the degree of ionization of the plasma, as shown in Table I. This increase, however, makes the semiclassical and other methods discussed here more applicable, because these methods are primarily designed for fully ionized plasmas.

Because the SC and RPA methods for calculating plasma electroconductivity are validated mostly for fully ionized plasmas, we have to estimate their applicability in the case of our experiments when certain amounts of neutral atoms were present. When the influence of neutral atoms is taken into account, the value of electroconductivity will change by the factor $f_{cor}=[1+(r_a^2/r_D^2)Q_{cor}(N_a/N_i)]^{-1}$, where r_a and r_D are the gas-kinetic radius of neutral atoms and Debye's radius, respectively. N_a and N_i are the densities of neutral atoms and ions, with $N_i=N_e$. Q_{cor} is the product of the inverse values of two factors. The first is found in the SC method and measures the influence of electron-electron scattering, with a value close to the corresponding Spitzer factor. The second factor takes into account the difference between Debye's radius and the screening radius used in the calculations. In the experimental conditions given here the calculated values of Q_{cor} are between 0.1 and 1. In the case of rare gases r_a is smaller than or close to the atomic length unit a_0. For $Q_{cor}\approx1$ and $r_a\approx a_0$ we have $f_{cor}\sim[1+(a_0^2N_a)/(r_D^2N_i)]^{-1}$. It can be shown that in the electron densities and temperature domains achieved in our experiments, f_{cor} differs significantly from 1 only if N_a is more than 10^4 times higher than N_e. Since this condition is not met in our plasma at any distance from the symmetry axis, the influence of electron-neutral scattering can be neglected.

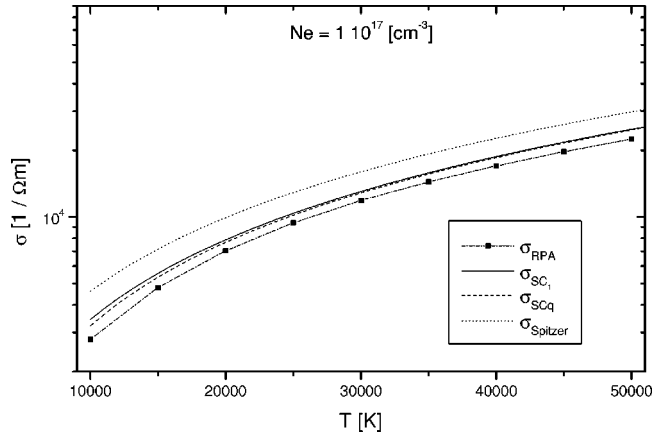

FIG. 6. The RPA, SC, and Spitzer plasma static conductivity as functions of temperature, when $N_e=10^{17}\ \mathrm{cm}^{-3}$. Subscripts SC_1 and SC_q refer to semiclassical calculations with $q=1$ and q from paper [7], respectively.

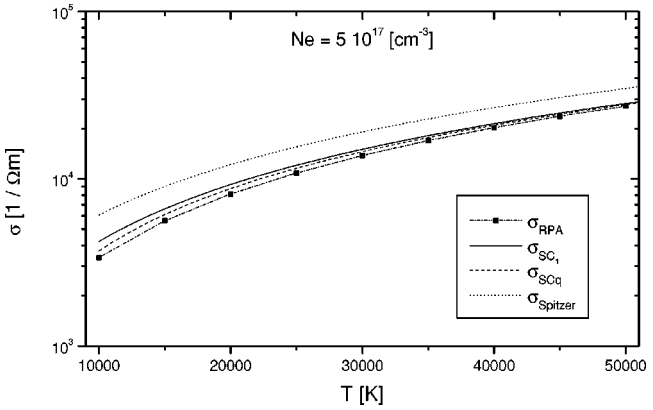

FIG. 7. Same as Fig. 6, but for $N_e=5\times10^{17}\ \mathrm{cm}^{-3}$.

These tables show the good agreement of the experimentally obtained impedance with the values calculated by Eq. (2) even in the case when $q=1$. A better agreement is achieved when the SC calculations are performed with $q=q(N_e,T)$ taken from [7]. The same tables contain the impedance values calculated by methods found in [6] and [8], and they are denoted here by Z_{Spitz} and Z_{Kur}, respectively. However, their agreement with Z_{expt} is much poorer.

It was shown in [2,3] that the RPA method gives good

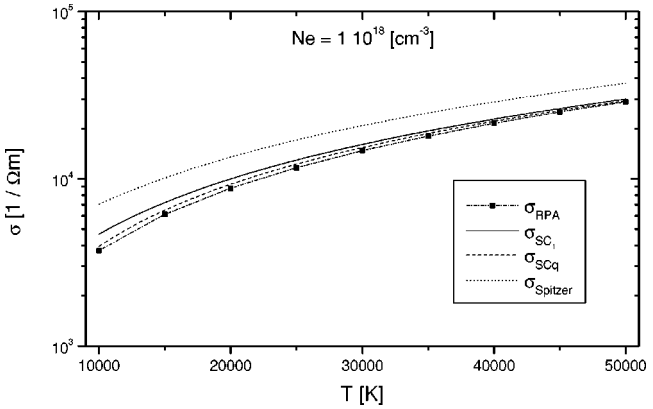

FIG. 8. Same as Fig. 6, but for $N_e=10^{18}\ \mathrm{cm}^{-3}$.

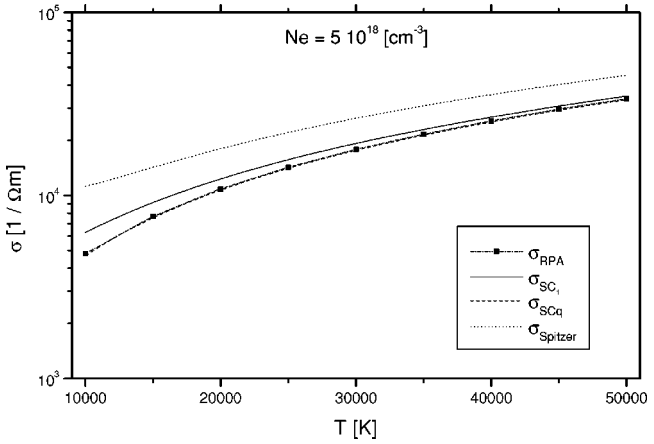

FIG. 9. Same as Fig. 6, but for $N_e = 5 \times 10^{18}$ cm^{-3}.

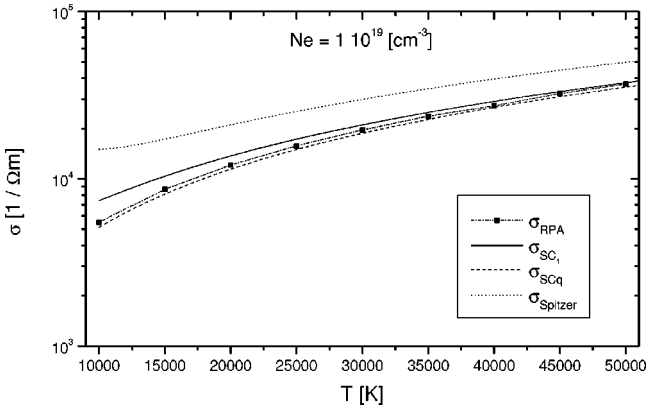

FIG. 10. Same as Fig. 6, but for $N_e = 10^{19}$ cm^{-3}.

results in the case of moderately dense plasmas at relatively high temperatures, and also in the case of very dense plasmas at relatively low temperatures. Using Eqs. (6) and (7), the calculated σ_{RPA} values in domains of $10^{17} \leqslant N_e \leqslant 10^{19}$ cm^{-3} and $10^4 \leqslant T \leqslant 5 \times 10^4$ K are represented in Table V. The SC static conductivity values calculated by Eq. (2) approximate the corresponding RPA values well, in N_e and T domains typical for practically important weakly and moderately nonideal laboratory plasmas. This is illustrated in Figs. 6–10 showing RPA and SC values (with a factor $q = 1$ and $q > 1$) for those domains of N_e and T values. The agreement is particularly good with the corrective factor q taken from [7]. The good agreement between the experimental results presented here and SC calculations confirms the validity of both RPA and SC methods, and also expands the region of their applicability.

It can be concluded that in the N_e and T domains mentioned above the plasma electroconductivity calculated by the RPA method is more accurate than the values obtained from Spitzer [6] and the method in [8]. This is not difficult to explain, because all phenomena considered in Spitzer's model (or in [8]) are also taken into account in the RPA method, but they are better described within the RPA method. An important example is the plasma inner electrostatic screening, which, unlike in the RPA method, is treated qualitatively in Spitzer's method.

Finally, it should be noted that in the domains of $N_e \sim 10^{18}$ cm^{-3} and $T \sim 2 \times 10^4$ K, the values of the small parameter s given by Eq. (8) are close to 0.4. Therefore, the agreement between experimental and calculated values implicitly confirms the validity of the RPA method for higher values of s, notably up to $s \sim 0.5$. Further investigation should show if this method is valid in cases when the parameter s is even closer to 1.

ACKNOWLEDGMENT

The authors would like to thank Professor V. M. Adamyan for his very useful discussions regarding the RPA method.

[1] A.A. Mihajlov, A.M. Ermolaev, Z. Djurić, and Lj. Ignjatović, J. Phys. D **26**, 1041 (1993).
[2] Z. Djurić, A.A. Mihajlov, V.A. Nastasyuk, M. Popović, and I.M. Tkachenko, Phys. Lett. A **155**, 415 (1991).
[3] V.M. Adamyan, Z. Djurić, A.M. Ermolaev, A.A. Mihajlov, and I.M. Tkachenko, J. Phys. D **27**, 111 (1994).
[4] Y. Vitel, M. El Bezzari, L.G. D'yachkov, and Y.K. Kurilenkov, Phys. Rev. E **58**, 7855 (1998).
[5] L.G. D'yachkov and P.M. Pankratov, J. Phys. B **24**, 2267 (1991); **27**, 461 (1994).
[6] L. Spitzer and R. Harm, Phys. Rev. **89**, 977 (1953).
[7] A.S. Kaklyugin and G.E. Norman, Teplofiz. Vys. Temp. **11**, 238 (1973).
[8] Yu.K. Kurilenkov and A.A. Valuev, Beitr. Plasmaphys. **24**, 161 (1984).